Article ID: 1001-3555(2017)05-0455-08

Synthesis of Indole-2-Carboxylic Ester Catalyzed by $Cu_2O/g\text{-}C_3N_4$

ZHU Zhu[1], LUO Mao-lan[2], ZHANG Jie[1], YANG Qin[2], ZHOU Li-mei[2*]

(1. *China West Normal University*, *Nan Chong* 637002, *China*;
2. *College of Chemistry and Chemical Engineering*, *China West Normal University*, *Nan Chong* 637002, *China*)

Abstract: The $Cu_2O/g\text{-}C_3N_4$ composite material was prepared by *in situ* reduction of Cu^{2+} absorbed on the surface defects of the $g\text{-}C_3N_4$, and characterized by XRD, SEM, FT-IR, and XPS. The XRD and XPS analysis revealed that Cu element was mostly doped in the $g\text{-}C_3N_4$ in the form of Cu_2O. The $g\text{-}C_3N_4$ and Cu_2O closely together can be described, according to all the characterization result. In addition, the obtained composite was employed as catalyst for one-pot three-step formation of indole-2-carboxylic esters, and achieved the middle yield (44.1%) under the low catalyst loading and mild condition.

Key words: $Cu_2O/g\text{-}C_3N_4$; heterogeneous catalysis; indole-2-carboxylic ester

CLC number: O643.32 **Document code**: A

The indole nucleus, recognized as a biologically significant moieties[1-4], has been the target of numerous synthetic methods[5-9]. Often, synthetic strategies introduced copper compounds to catalyze the indole derivatives formation reaction in excellent yields[10-12], and proceeded via a presumed mechanism (Scheme 1). Unfortunately, many of these transformations applied to the indole ring system need a high dosage of copper catalyst, give merely moderate yields (34% ~ 53%)[10-11] and are not favorable for the sufficient separation of catalysts and/or products. Overall, it would not be most welcome from atom-economy and environment perspective.

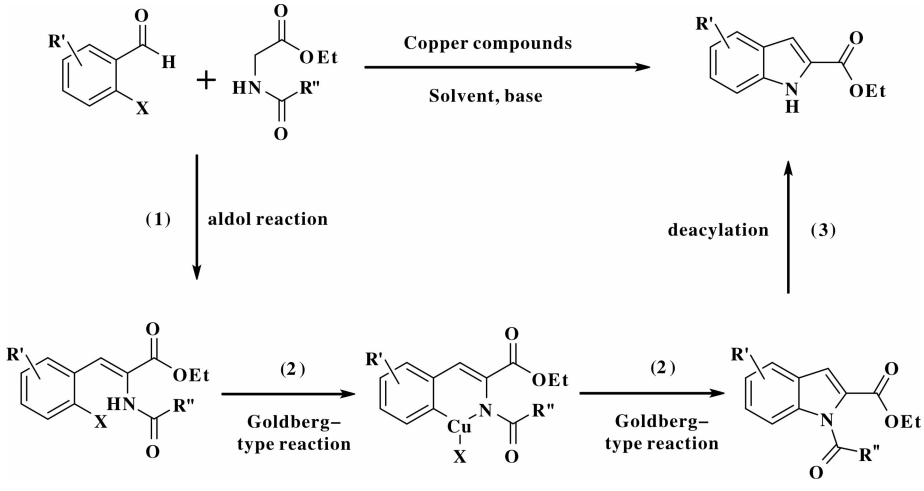

Scheme 1 The plausible mechanism of indole formation

Received date: 2017-05-28; **Revised date**: 2017-06-20.

Foundation: The Natural Science Foundation of China (21303139).

First author: ZHU Zhu (1989-), female, graduate student. E-mail: zhangjie200610183@126.com.

Corresponding author: E-mail: cwnuzhoulimei@163.com.

Graphitic carbon nitride (g-C_3N_4) as a sort of polymeric super molecular materials exhibits excellent stability as well as good environmental acceptance. The surface of g-C_3N_4 contains a small amount of hydrogen present as primary and/or secondary amine groups on the terminating edges, which can form a quantity of surface defects along with its unique dimensional layered structure. It is favorable for hybridizing with other components, due to this structure fragment and the electronic properties (a larger size of the π system). Accordingly, g-C_3N_4 features almost the precursor of transition metal heterogeneous catalyst[13-16]. Herein, we would like to synthesize the Cu_2O/g-C_3N_4 on the pioneering work of predecessor, and utilize it to catalyze the formation of indole-2-carboxylic esters in order to avoid catalyst's separation problems, the low yields and the high loading of catalyst, starting from 2-bromobenzaldehyde and ethyl acetamidoacetate.

1 Experimental section

1.1 Preparation of the g-C_3N_4 polymeric materials

Firstly, melamine (2.5 g) powder was put into a semi-closed alumina crucible with a cover under N_2 gas flow to 550 ℃ for 4 h at a heating rate of 5 ℃/min, followed by naturally cooling to room temperature. After cooling, the yellow product was milled and collected.

1.2 Preparation of the Cu_2O/g-C_3N_4 composite

0.2 g of g-C_3N_4 and 0.075 g of $CuCl_2 \cdot 2H_2O$ were ultrasonically dispersed in 100 mL mixture solution of H_2O/EtOH (the volume rate is 1∶1) for 1.5 h, and 100 mL of aqueous solution containing 0.165 8 g of $NaBH_4$ was added dropwise under stirring at 25 ℃. The yellow-brown solution changed gradually to deep blue within 0.5 h. Then the deep blue solution was stirring for 16 h. The product were centrifuged and washed with distilled water and EtOH for several times, and dried in a vacuum oven at 60 ℃. The brown product was obtained in 0.23 g.

1.3 Characterization

The X-ray diffraction patterns of the Cu_2O/g-C_3N_4 and the g-C_3N_4 were recorded by diffractometer (D/MAX Ultima IV, Rigaku, Japan). The X-ray photoelectron spectroscopy spectra were examined on the X-ray energy spectromer (Kratos Analytical Axis Ultra, United Kingdom). Fourier transform infrared spectroscopy spectra were scanned on the Nicolet-6700 spectrometer. SEM measurements were carried out by the JSM-6510LV scanning electron microscopy (Rigaku, Japan).

1.4 General procedure for indole-2-carboxylic esters

Caesium carbonate (652 mg, 2 mmol) and catalyst (30 mg) were added to a dried reaction tube. The tube was filled with nitrogen before DMSO (2 mL) was added. Then 2-bromobenzaldehyde (185 mg, 1 mmol) and ethyl acetamidoacetate (156.2 mg, 1.2 mmol) were added prior to heating the slurry to 100 ℃ under a nitrogen atmosphere for 12 h with good agitation. After cooled down, the mixture was added DI water (5 mL) and extracted with ethyl acetate (5 mL) for 3 times. The combined organic fraction was washed with DI water (5 mL) and brine (5 mL). After dried over sodium sulfate and filtered, the organic phase was concentrated to give crude product. The crude product was further analyzed by GC Agilent 7890A gas chromatography using HP-5 column (30 m × 0.32 mm × 0.25 μm) and FID detector

2 Results and Discussion

Schematic illustration of the synthesis process of the Cu_2O/g-C_3N_4 composite is indicated in Scheme 2. The first step requires the calcination of melamine at high temperature to obtain the entitled product (g-C_3N_4). The second step is the adsorbing of Cu^{2+} on the surface defects of g-C_3N_4 with the addition of $CuCl_2 \cdot 2H_2O$. The third step is the reduction reaction of Cu^{2+} under the presence of reducing agent.

The actual images of the Cu_2O/g-C_3N_4 and g-C_3N_4 are exposed in Fig. 1. The g-C_3N_4 is off-white powder. Compared to g-C_3N_4, the Cu_2O/g-C_3N_4 is a small fulvous block-liker, which suggests that Cu_2O is successfully adsorbed on the surface defects of g-C_3N_4 from the facade of the prepared product.

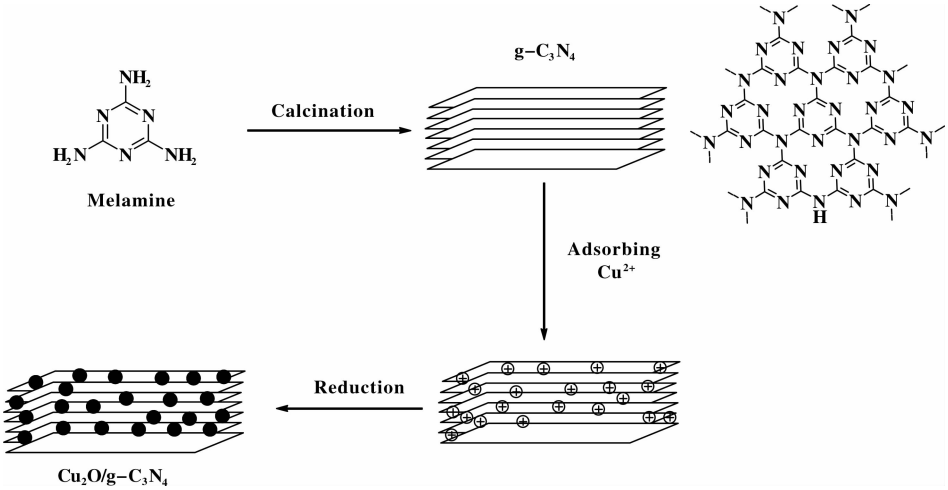

Scheme 2 Illustration of the preparation of $Cu_2O/g\text{-}C_3N_4$

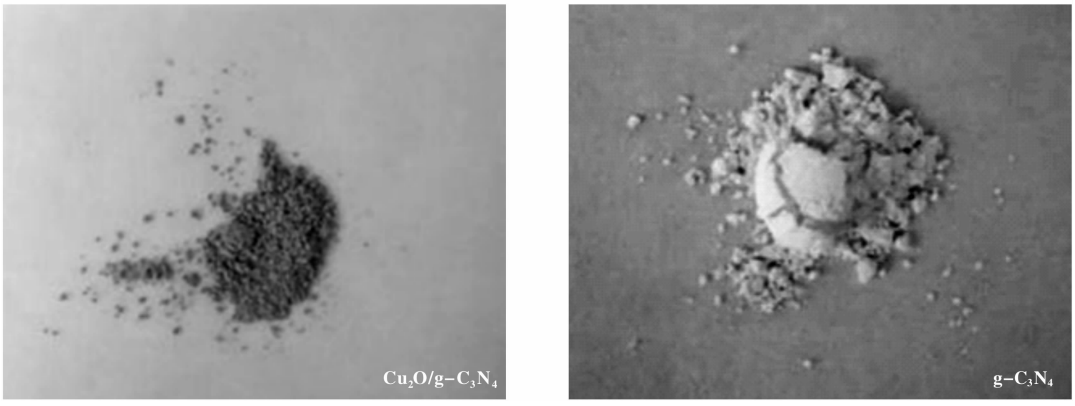

Fig. 1 The digital photographs of the $Cu_2O/g\text{-}C_3N_4$ and $g\text{-}C_3N_4$

As shown in Fig. 2, the FTIR spectrum of the $Cu_2O/g\text{-}C_3N_4$ is similar with that of the $g\text{-}C_3N_4$, because of no characteristic peak of Cu_2O. The peak at 810 cm^{-1} is attributed to out of bending modes C-N heterocycles, while the peak between 1 250 and 1 650 cm^{-1} are assigned to aromatic C=N and C-N stretching vibration. The measurement result is correspond to the reported literature[17].

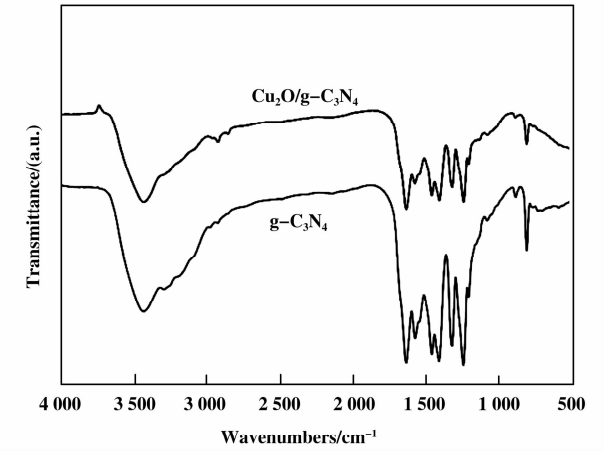

Fig. 2 Fourier transform infrared spectroscopy of the $Cu_2O/g\text{-}C_3N_4$ and $g\text{-}C_3N_4$

XRD and XPS analysis were performed to further confirm the formation of the $Cu_2O/g\text{-}C_3N_4$. The full range XPS spectrum of $Cu_2O/g\text{-}C_3N_4$ (Fig. 3) reveals that the composite contains C, N, O, and Cu element. It was clear that the peak appearing at 530.6 eV implied the presence of O^{2-} and the peak at 287.9 eV was attributed to the carbon of C—C, while the characteristic peak at 932.6 , 952.5 eV were assigned to Cu^{+}[18-20].

The diffraction peaks of $Cu_2O/g\text{-}C_3N_4$, Cu_2O and pure Cu can be observed simultaneously, according to the information provided by the schematic diagram (Fig.4). The peak's intensity (at 42.2°, 61.6°,

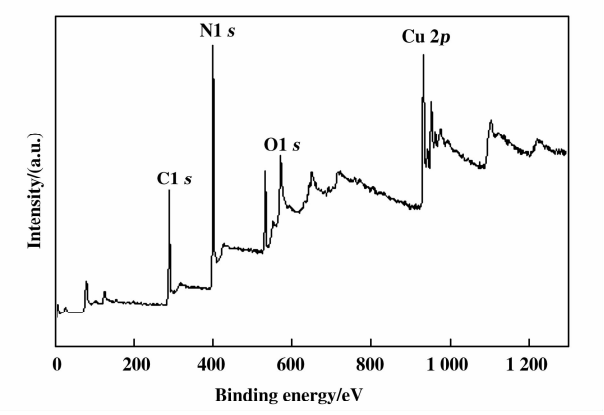

Fig. 3 The full range XPS spectrum of $Cu_2O/g\text{-}C_3N_4$

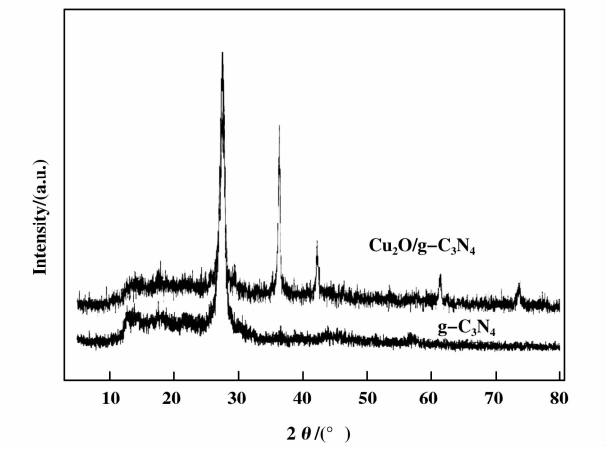

Fig. 4 The XRD spectra of $Cu_2O/g\text{-}C_3N_4$ and $g\text{-}C_3N_4$

73.6°) of pure Cu is much weaker than that (at 37.7°) of Cu_2O, which reveals the presence of a light amount of pure Cu. The high intensity peak located at 27.6° is corresponded to the pure $g\text{-}C_3N_4$, which is in accordance with previous report[21].

Additionally, SEM measurement was performed to investigate the microstructure of the $Cu_2O/g\text{-}C_3N_4$ and $g\text{-}C_3N_4$. From the SEM image (Fig. 5A) of $g\text{-}C_3N_4$, it can be seen that the g - C_3 N_4 appears the sheet spatial

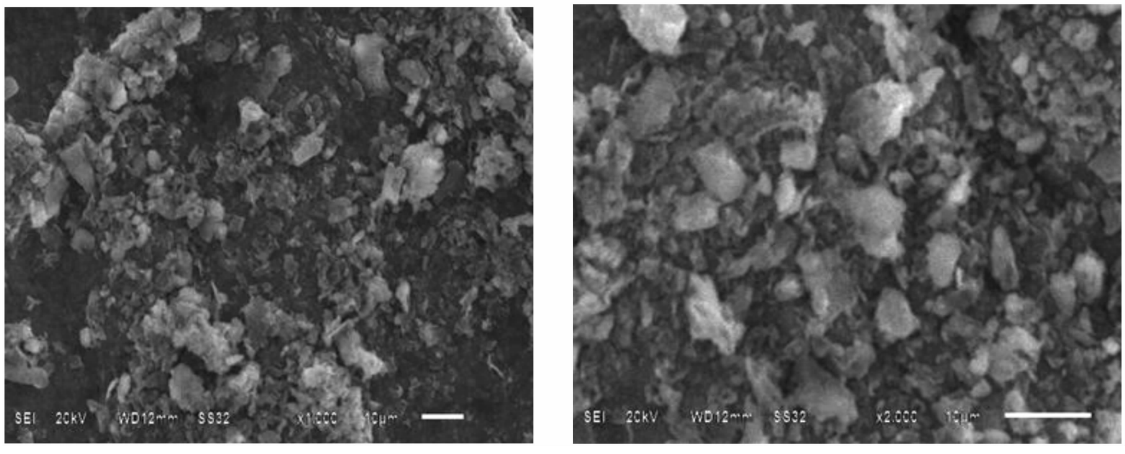

Fig. 5 SEM image A of the $g\text{-}C_3N_4$ and SEM image B of the $Cu_2O/g\text{-}C_3N_4$

structure and bending aggregation. It is visible from Fig. 5B that the appearance characteristics of $g\text{-}C_3N_4$ are modified, which is caused by the adsorption of numerous Cu_2O. All of these measurement results can confirm that the prepared sample is the $Cu_2O/g\text{-}C_3N_4$ composite though there is a trace amount of pure copper.

During the course of work, we set out to research the catalytic potentiality of $Cu_2O/g\text{-}C_3N_4$ for the synthesis of indole-2-carboxylic esters, using 2-bromobenzaldehyde and ethyl acetamidoacetate as reaction substrates in DMSO. To begin with, what is investigated that the catalytic efficiency of this transformation is affected by the embedded quantity of Cu in the case of the $Cu_2O/g\text{-}C_3N_4$ particles (see Table 1).

A low yield of 7.70% and 13.5% was obtained when the reaction was proceeded with the pure $g\text{-}C_3N_4$ and Cu_2O respectively (Table 1, entry 5 and 6). Meanwhile, the mixture of Cu_2O and Cu gave the yield of 8.20% (Table 1, entry 7). As anticipated, the catalytic activity of this reaction was improving as the loading of Cu increasing until 12.3% in the case of the $Cu_2O/g\text{-}C_3N_4$ (Table 2, entries 1 - 4). So, the Cu loading (12.3%) of the $Cu_2O/g\text{-}C_3N_4$ was selected as

Table 1 Screening of condition with the loading of Cu in the case of the $Cu_2O/g\text{-}C_3N_4$[a]

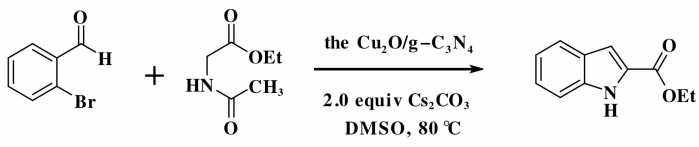

Entry	Catalyst	Cu loading/%	Time/h	Yield/%[b]
1	$Cu_2O/g\text{-}C_3N_4$	7.50	12	17.2
2	$Cu_2O/g\text{-}C_3N_4$	10.0	12	23.8
3	$Cu_2O/g\text{-}C_3N_4$	12.3	12	35.9
4	$Cu_2O/g\text{-}C_3N_4$	17.5	12	12.8
5	$g\text{-}C_3N_4$	–	12	7.70
6	Cu_2O[c]	–	12	13.5
7	Cu_2O/Cu[d]	–	12	8.20

a. reaction conditions: 2-bromobenzaldehyde (1 mmol), ethyl acetamidoacetate (1.2 mmol), the $Cu_2O/g\text{-}C_3N_4$ (20 mg), Cs_2CO_3 (2.0 equiv), DMSO (2 mL), 80 ℃; b. Yield determined by GC; c. 5.50 mg Cu_2O; d. 4.0 mg Cu_2O, 1.5 mg Cu.

Table 2 Probing condition of base and solvent for this transformation[a]

Entry	Solvent	V/mL	Base	Equiv	Yield/%[b]
1	DMSO	2	Cs_2CO_3	2.0	35.9
2	NMP	2	Cs_2CO_3	2.0	10.0
3	Toluene	2	Cs_2CO_3	2.0	8.60
4	1, 4 - dioxane	2	Cs_2CO_3	2.0	8.10
5	Ethyl acetate	2	Cs_2CO_3	2.0	31.5
6	DMF	2	Cs_2CO_3	2.0	6.70
7	1-decanol	2	Cs_2CO_3	2.0	0
8	DMSO	2	K_2CO_3	2.0	19.7
9	DMSO	2	K_3PO_4	2.0	9.20
10	DMSO	2	CH_3COONa	2.0	trace
11	DMSO	2	LiOH	2.0	6.30
12	DMSO	2	KOH	2.0	3.00
13	DMSO	2	NaOH	2.0	10.6
14	DMSO	2	$KHCO_3$	2.0	2.60
15	DMSO	2	Cs_2CO_3	1.5	26.0
16	DMSO	2	Cs_2CO_3	2.5	26.8

a. Reaction conditions: 2-bromobenzaldehyde (1 mmol), ethyl acetamidoacetate (1.2 mmol), the $Cu_2O/g\text{-}C_3N_4$ (20 mg, 3.8 mmol % Cu), 80 ℃; b. Yield determined by GC.

the heterogeneous catalyst in the following investigation. After examining of the effects of various embedded amount of Cu, various bases and reaction media were explored. Following the bases and solvents screen (Table 2), we found no reaction took place at all using 1-decanol as solvent (Table 2, entry 7). Meanwhile, a trace amount of the desired product was observed in the DMF which was proven to be preferable solvent for this reaction[10]. Other solvents such as NMP, Toluene, 1,4-dioxane failed to provide more than a trace amount of the desired products (Table 2, entries 2-4). To our delight, the yield still resulted in 35.9% and 31.5% respectively when DMSO and Ethyl acetate were employed as the solvent (Table 2, entries 1 and 5). Subsequently, the influence of the base was evaluated in DMSO. A series of base (K_2CO_3, K_3PO_4, CH_3COONa, LiOH, KOH, NaOH, $KHCO_3$) were investigated in the reaction, and we found that the screened base (Cs_2CO_3), giving good yield (35.9%), was preferred for this transformation (Table 2, entry 1 vs entries 8-14). A slight decrease in the amount of Cs_2CO_3 resulted in an obvious decrease in the yield of the desired product (Table 2, entry 15). Considering the moderate basicity, we chose Cs_2CO_3(2 equiv) as base in the formation of indole-2-carboxylic esters.

Furthermore, we attempted to investigate the influence of reaction temperature and the catalyst loading (the Cu_2O/g-C_3N_4) in the transformation. As seen in Table 3, the yields were found to increase with a raising in the temperature (Table 3, entries 1-3) although the condition of high temperature (120 ℃) retarded the reaction (Table 3, entry 4). In the case of catalyst (the Cu_2O/g-C_3N_4) dosage, the experiments performed similarly with that of the temperature: increasing the dosage of the Cu_2O/g-C_3N_4 composite improved the yield of the reaction (Table 3, entries 3, 5-6). Surprisingly, the high dosage (40 mg) of catalyst led to a slight decrease in the yield (Table 3, entry 7). From what has been discussed above, the optimal condition of the one-pot three-step formation of indole-2-carboxylic esters is refined as follow: the Cu_2O/g-C_3N_4(30 mg, 5.8% Cu), Cs_2CO_3(2.0 equiv), DMSO (2 mL) and 100 ℃.

Table 3 Optimizingreaction temperature and the amount of catalyst[a]

Entry	Catalyst/mg	Temp/℃	Yield/%[b]
1	20[c]	60	31.4
2	20[c]	80	35.9
3	20[c]	100	40.0
4	20[c]	120	21.7
5	10[d]	100	25.1
6	30[f]	100	44.1
7	40[e]	100	41.7

a. Reaction conditions: 2-bromobenzaldehyde (1 mmol), ethyl acetamidoacetate (1.2 mmol), Cs_2CO_3(2.0 equiv), DMSO (2 mL); b. Yield determined by GC; c. Cu_2O/g-C_3N_4(20 mg, 3.8 mmol% Cu); d. Cu_2O/g-C_3N_4(10 mg, 1.9 mmol% Cu); f. Cu_2O/g-C_3N_4(30 mg, 5.8 mmol% Cu); e. Cu_2O/g-C_3N_4(40 mg, 7.6 mmol % Cu).

With our reaction conditions refined in hand, we further probed the scope of this novel methodology. Thus, a series of starting substrates were subjected to the reaction in DMSO (Table 4). All of benzaldehydes containing electron-rich groups reacted to give the expected indole product in the range of 30.6% ~34.4% yield (Table 4, entries 5 and 6), while electron-poor substrates did not react well with this system (Table 4, enties 2-4).

Table 4 Synthesis of Various Heterocycle-2-carboxylic Esters[a]

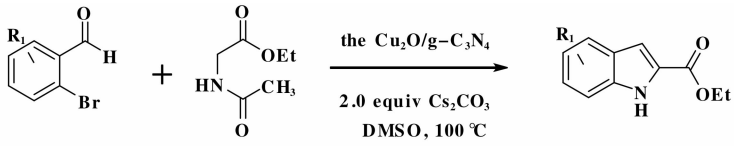

Entry	Starting material 1	Starting material 2	Desired product	Yield/%[b]
1	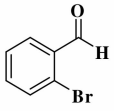	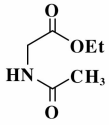	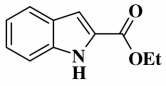	44.1
2	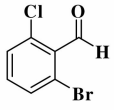	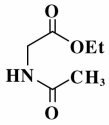	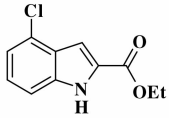	13.2
3	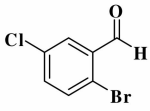	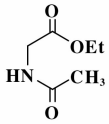	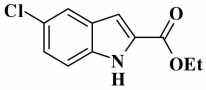	13.5
4	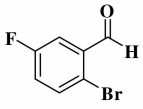	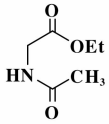	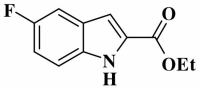	10.1
5	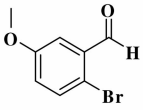	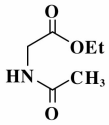	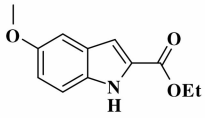	30.6
6	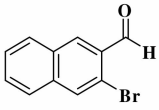	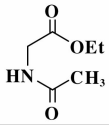	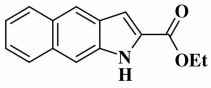	34.4

a. Reaction conditions: 2-bromobenzaldehyde (1 mmol), ethyl acetamidoacetate (1.2 mmol), the $Cu_2O/g\text{-}C_3N_4$ (30 mg, 5.8 mmol% Cu), 100 ℃, Cs_2CO_3 (2.0 equiv), DMSO (2 mL); b. Yield determined by GC.

3 Conclusion

In summary, the $Cu_2O/g\text{-}C_3N_4$ composite was synthesized by the calcination of melamine, ultrasonic exfoliation, and reduction of Cu^{2+} adsorbed on the defects of $g\text{-}C_3N_4$, and characterized by FTIR, XRD, XPS and SEM. Meanwhile, the $Cu_2O/g\text{-}C_3N_4$ was utilized to catalyze the formation of indole-2-carboxylic esters and gave desired yield although the low dosage (30 mg, 5.8% Cu) of catalyst was used. To the best of our knowledge, this procedure has not been reported to date.

References:

[1] Biersack B, Schobert R. Indole compounds against breast canser: Recent development [J]. *Curr Drug Targets*, 2012, **13**(14): 1705-1719.

[2] Kaushik N K, Attri P, Kumar N, *et al*. Biomedical importance of indoles [J]. *Molecules*, 2013, **18**(6): 6620-6662.

[3] Brewer M R, Pao W. Maximizing the benefits of off-target kinase inhibitor activity[J]. *Cancer Discov*, 2013, **3**(2): 138-140.

[4] Ahmad A, Sakr W A, Rahman K M. Mechanisms and therapeutic implications of cell death induction by indole compounds[J]. *Cancers*, 2011, **3**(3): 2955-2974.

[5] Inman M, Moody C J. Indole synthesis-Something old, something new [J]. *Chem Sci*, 2013, **4**(1): 29-41.

[6] Shi Z, Glorious F. Efficient and versatile synthesis of indoles from enamines and imines by cross-dehydrogenative coupling [J]. *Angew Chem Int Ed*, 2012, **51**(37):

9220-9222.

[7] Taber D F, Tirunahari P K. Indole synthesis: A review and proposed classification[J]. *Tetrahehdron*, 2011, **67**(38): 7195-7210.

[8] Cacchi S, Fabrizi G, Goggiamani A. Indoles via palladium catalyzed cyclization[J]. *Org Rea*, 2012, **76**(4): 281-534.

[9] McNulty J, Keskar K. A tandem "on-palladium" Heck-Jeffery amination route toward the synthesis of functionalized indole-2-carboxylates [J]. *Eur J Org Chem*, 2011, **34**(34): 6902-6908.

[10] Stefan G K, John W D, Yan B L, *et al.* A ligand-free, copper-catalyzed cascade sequence to indole-2-carboxylic esters [J]. *Tetrah*, 2010, **51**(50): 6549-6551.

[11] Stefan G K, John W D, Yan B L, *et al.* Copper-Catalyzed synthesis of indoles and related heterocycles in renewable solvents[J]. *ACS Sust Chem Eng*, 2014, **2**(6): 1359-1363.

[12] David S S, Stephen L B. Diamine ligands in copper-catalyzed reactions[J]. *Chem Sci*, 2010, **1**(1): 13-31.

[13] a. Zhu H, Chen X, Zhao J C, *et al.* Mechanism of supported gold nanoparticles as photocatalysts under ultraviolet and visible light irradiation [J]. *Chem Commun*, 2009, **48**(48): 7524-7526.

b. He Ping(何 平), Chen Yong(陈 勇), Fu Wen-fu(傅文甫). Study of visible-light driven preparation of Fe/g-C_3N_4 composite catalyst with simultaneous hydrogen evolution(可见光驱动制备 Fe/g-C_3N_4 复合催化剂及其产氢研究)[J]. *J Mol Catal*(*China*)(分子催化), 2016, **30**(3): 269-275.

c. Ma Lin(马 琳), Kang Xiao-xue(康晓雪), Hu Shaozheng(胡绍争), *et al.* Preparation of Fe, P CodopedGraphitic carbon nitride with enhanced visible-light photocatalytic activity(Fe-P 共掺杂石墨相氮化碳催化剂可见光下催化性能研究)[J]. *J Mol Catal*(*China*)(分子催化), 2015, **29**(4): 359-368.

[14] Vien V, Nguyen V K, Sung J K, *et al.* Preparation of g-C_3N_4/Ta_2O_5 composites with enhanced visible light photocatalytic activity [J]. *Elect Mater*, 2016, **45**(5): 2334-2340.

[15] Yong C B, Ke Z C. AgCl/Ag/ g-C_3N_4 hybrid composites: preparation, visible light-driven photo catalytic activity and mechanism [J]. *Nano Micro Lett*, 2016, **8**(2): 182-192.

[16] Yasir A, Qun H, Dao B L, *et al.* Facile synthesis of mesoporous detonation nanodiamond-modified layers of graphitic carbon nitride as photocatalysts for the hydrogen evolution reaction [J]. *RSC Adv*, 2017, **7**(25): 15390-15396.

[17] Ge L. Synthesis and photocatalyic performance of novel metal-free g-C_3N_4 photocatalyst[J]. *Mater Lett*, 2011, **65**(17/18): 2652-2654.

[18] Zou S W, How C W, Chen J P. Photocatalytic treatment of wastewater contaminated with organic waste and copper ions from the semiconductor industry[J]. *Ind Eng Chem Res*, 2007, **46**(2): 6566-6571.

[19] Spasiano D, Rodriguez L D P, Olleros J C, *et al.* TiO_2/Cu(II) photocatalytic production of benzaldehyde from benzyl alcohol in solar pilot plant reactor[J]. *Appl Catal B*, 2013, **56**(5): 136-137.

[20] Chusshuei C C, Brookshier M A, Goodman D W. Correlation of relative X-way photoelectron spectroscopy shake-up intensity with CuO partcile size [J]. *Langmuir*, 1999, **15**(8): 2806.

[21] X Wang, K Maeda, A Thomas, *et al.* A metal-free polymeric photocatalyst for hydrogen production from water under visible light [J]. *Nat Mater*, 2009, **8**(1): 76-80.

Cu_2O/g-C_3N_4 催化合成吲哚-2-羧酸酯

朱 珠[1], 罗贸兰[2], 张 杰[1], 杨 琴[2], 周丽梅[2*]

(1. 西华师范大学, 四川 南充 637002;
2. 西华师范大学 化学化工学院, 四川, 南充 637002)

摘要: 我们通过原位还原的方法将吸附在 g-C_3N_4 表面上 Cu^{2+}还原, 制备出 Cu_2O/g-C_3N_4 复合材料, 并利用 XRD、SEM、FT-IR、XPS 等分析手段表征 Cu_2O/g-C_3N_4. 表征结果显示: Cu 元素主要以 Cu_2O 的形式吸附在 g-C_3N_4 载体上. 另外, 还考察了 Cu_2O/g-C_3N_4 在"一锅法"合成吲哚-2-甲酸乙酯的反应中的催化性能. 结果表明: 即使在较低的催化担载量和温和的反应条件下, Cu_2O/g-C_3N_4 仍能表现出良好的催化性能并获得 44.1 % 的收率.

关键词: Cu_2O/g-C_3N_4; 多相催化; 吲哚-2-羧酸酯